



A CW, 94 GHz Second Harmonic Gyrotron with a Continuous Operation Solenoid Cooled by Water

Dimin Sun¹ · Qili Huang¹ · Linlin Hu¹ · Tingting Zhuo¹ · Guowu Ma¹ · Hongbin Chen¹ · Fanbao Meng¹

Received: 15 May 2021 / Accepted: 16 August 2021 / Published online: 23 December 2021

© The Author(s), under exclusive licence to Springer Science+Business Media, LLC, part of Springer Nature 2021

Abstract

Design and experimental results of a continuous wave (CW), 94 GHz second harmonic gyrotron with a 1.8 T continuous operation solenoid are presented. In order to reduce power consumption of the solenoid, a carbon steel shell was designed to concentrate the magnetic flux into the gyrotron cavity region. The inner hole is 66 mm in diameter. That is big enough to insert a CW, medium power gyrotron. When driven by a current of 476 A, maximum magnetic field of 1.8 T in the cavity region was detected and the power consumption was 25 kW. The solenoid was cooled effectively with a water flow of 1.5 L/s. Based on the 1.8 T solenoid, a compact triode magnetron injection gun (MIG) was used to generate gyrating electron beam for the second harmonic gyrotron. The gyrotron operated at the TE_{0,2} mode with a conventional cylindrical cavity. And a high-efficiency quasi-optical mode converter with a dimpled-wall launcher was designed, the mode conversion efficiency was 97%, and the Gaussian content of the output beam was 98%. During the CW test, continuous operation of 5 min was realized. Its operational frequency stabilized at 93.9 GHz. The output power was 12 kW with an electron beam of 45 kV, 1.6 A. The output efficiency was 24% with a single-stage depressed collector.

Keywords Gyrotron · Harmonic · Millimeter wave · Solenoid · W-band

1 Introduction

Gyrotrons are powerful sources at millimeter and submillimeter waves. They are important for numerous applications such as material processing [1], plasma diagnostics [2], electron cyclotron resonance heating and electron cyclotron current drive in thermonuclear fusion research [3–5], electron-spin resonance experiments [6], and nuclear magnetic resonance spectroscopy enhanced by dynamic nuclear polarization [7, 8]. Particularly, W-band CW

✉ Guowu Ma
hunter_ma@126.com

¹ Institute of Applied Electronics, China Academy of Engineering Physics, Mianyang 621900, China

gyrotrons could be used as power sources for the non-lethal active denial system (ADS) [9]. The required operating frequency of ADS is about 94 GHz.

The operating frequency of a gyrotron is close to the cutoff frequency of a TE mode in an overmoded cavity, which is situated in an external static magnetic field. According to the synchronism condition, the operating frequency of a gyrotron can also be close to a harmonic s of the electron cyclotron frequency in the interaction region. The following two conclusions can be drawn. First, very high magnetic field in the cavity region is required for millimeter and submillimeter wave gyrotrons operating at the fundamental harmonic ($s = 1$) of the electron cyclotron frequency. Second, the magnetic field required for a gyrotron can be reduced by a factor of s ($s > 1$) when operating at the s th harmonic of the electron cyclotron frequency. For example, the peak magnetic field required for a W-band gyrotron operating at the fundamental harmonic is about 3.6 T and the only possible option for CW operation is to use a superconducting magnet. The cost is high and it is not suitable for use on vehicle platform. For a third harmonic gyrotron operating at W-band, the magnetic field value required is only 1.2 T. Both permanent magnets and direct current (DC) solenoids are able to satisfy the demands. However, severe mode competition often precludes the desired high harmonic mode from oscillating.

The second harmonic gyrotron operating at W-band requires the peak magnetic field to be 1.8 T. There are two candidates for generating the magnetic field, superconducting magnets and DC solenoids. Certainly, we do not want a W-band second harmonic gyrotron with a superconducting magnet because it has no advantages over the fundamental one. And for a conventional solenoid which can produce 1.8 T magnetic field, the power consumption is too high. It is really difficult to cool the solenoid.

But, if we can find a new method to reduce the power consumption to an acceptable level, W-band second harmonic gyrotrons can probably become more competitive since one can get rid of superconducting magnets and the mode competition is mild.

Fortunately, we can find the method. In 2014, D. Borodin [10] designed and tested a continuous operation copper solenoid, which can produce 1.8 T magnetic field for a 95 GHz second harmonic gyrotron. In order to reduce the power consumption, an iron shell was used to concentrate the magnetic flux into the cavity region. The power consumption is expected to stabilize at only 25 kW. Long pulse operation of a second harmonic gyrotron based on this solenoid has been realized. The output peak power of the gyrotron was about 33kW at 3.2A beam current, with efficiency of 23% [11, 12]. However, the minimum radius of the copper foil is only 7.5 mm. It is really a challenge to use this solenoid for a hard sealed CW gyrotron with an internal quasi-optical mode converter.

Recently, we have successfully tested a hard sealed, 94 GHz, CW second harmonic gyrotron with a wide bore, continuous operation solenoid [13]. In this manuscript, design and test results are presented. In the next section, the design and test results of the solenoid are described. The design of a W-band second harmonic gyrotron based on the solenoid is presented in Section 3. In Section 4, we present the test results of the second harmonic gyrotron. At last, we summarize the work and discuss future directions.

2 Design and Experimental Results of the 1.8 T Solenoid

In order to reduce power consumption, ferromagnetic material can be used to concentrate the magnetic flux into the gyrotron cavity region. Since we aimed to design a CW gyrotron with

an internal quasi-optical mode converter, the solenoid consists of two parts. The main part generates the high magnetic field required for beam-wave interaction in the cavity, while the additional part produces a magnetic field to keep the gyrating electron beam away from the dimpled-wall launcher. The optimized structure of the solenoid is shown in Fig. 1.

Steel type Q235 (corresponding to ST37) was chosen as the shell material. The B-H curve of this steel is shown in Fig. 2. The thickness of the outer shell is 30 mm to ensure that the shell is not saturated. Unlike the solenoid designed by D. Borodin, the homogeneity was realized by use of the inner shell instead of additional correction coils [10]. A wide bore can be achieved by this method. Another advantage of this method is that the field homogeneity is not sensitive to current changes.

The main part of the solenoid is comprised of 9 concentric cylindrical segments of copper foil windings, while the additional part includes 4 cylindrical segments. Each of the segments contains 30 layers of copper foil. In each layer, there are a 0.3-mm-thick copper foil and a 0.05-mm-thick polyimide insulation foil. It is not realistic to avoid assembly errors during the process of winding. And, for convenience, an adhesive layer between the copper and polyimide is necessary. Therefore, the total thickness of a single layer was set as 0.42 mm in the simulation. That is reasonable according to the actual conditions. The final solenoid data is detailed in Table 1. When calculating the resistance of the segments, the average temperature of the copper foils is treated as 30 °C.

Between adjacent segments, the gap width is 5 mm, in which water is pumped for cooling. And between the segments and the steel shell, there is a gap of 5 mm for cooling water channels and supporting structures. The supporting structures also serve as insulation structures.

To obtain a wide bore, we can split the innermost parts from the carbon steel shell and fix them on the gyrotron tube. The two innermost segments (#1 and #10) have the same inner radius of 40 mm. It is possible to realize a wide bore with a diameter of 66 mm at the center of the solenoid that is wide enough for a medium power W-band, CW gyrotron.

Fig. 1 Simulation model of the solenoid

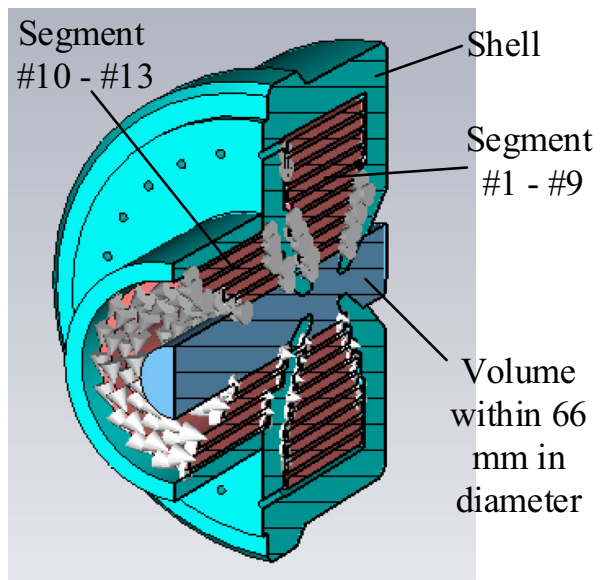
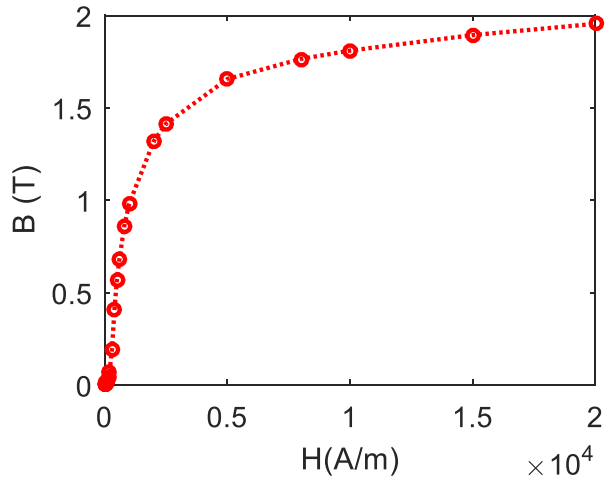


Fig. 2 The B-H curve of steel type Q235



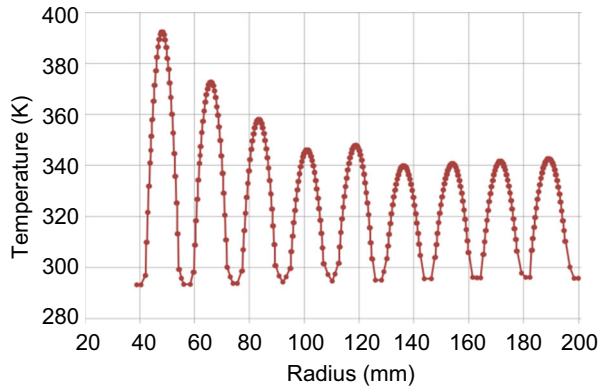
For a current of 476 A, the maximum magnetic field reaches 1.8 T in the cavity region. The field homogeneity is $\pm 0.3\%$ over a length of 26 mm. With the help of the additional part of the solenoid, 0.5 T magnetic field can be generated in the dimpled-wall launcher. The average radius of the launcher is 7 mm. And the gyrating electron beam can be kept 2 mm in distance from the wall.

For a current of 476 A, the power consumption of the main part and the additional part is 20.4 kW and 6.0 kW, respectively. The total power consumption is 26.4 kW. This solenoid can be cooled with water. When the water flow rate is 1.5 L/s, the radial temperature distribution in the main part is shown in Fig. 3. The maximum temperature is 394 K in segment #1. The global maximum temperature is 405 K near the end of segment #1. This is not a problem since the melting temperature of polyimide is above 250 °C. Except segment #1 and segment #2, the temperature inside copper foils is below 100 °C. Since the power consumption density is lower, the additional part can also be cooled effectively with a water flow of 1.5 L/s.

Table 1 Solenoid characteristics

Segment #	Turns	Width	Rin (mm)	Rout (mm)	Resistance (mΩ)
1	30	80	40.0	52.6	6.98
2	30	100	57.6	70.2	7.71
3	30	120	75.2	87.8	8.19
4	30	140	92.8	105.4	8.54
5	30	140	110.4	123.0	10.06
6	30	160	128.0	140.6	10.13
7	30	160	145.6	158.2	11.45
8	30	160	163.2	175.8	12.78
9	30	160	180.8	193.4	14.11
10	30	100	40.0	52.6	5.59
11	30	120	57.6	70.2	6.42
12	30	140	75.2	87.8	7.02
13	30	160	92.8	105.4	7.47

Fig. 3 The radial temperature distribution in the main part (Segment #1–#9)

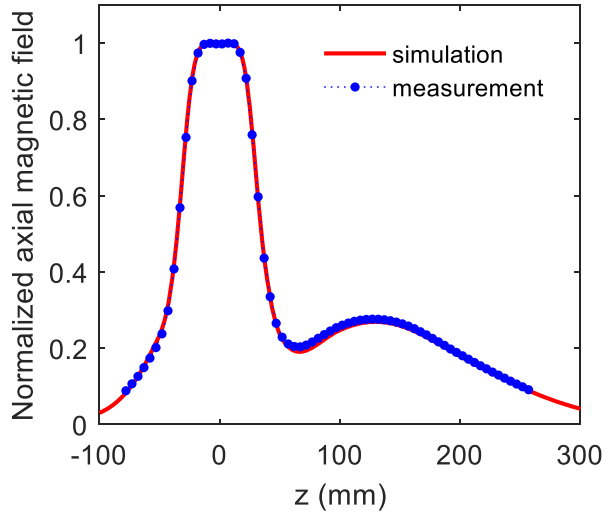


According to the design results, we have made a prototype of the solenoid, as shown in Fig. 4. The solenoid is 530 mm in diameter, and 450 mm in height. When a DC current of 476 A was driven through the copper foils, maximum magnetic field of 1.811 T in the cavity region was detected. The normalized magnetic field profile is shown in Fig. 5. At $z = 70$ mm, the axial magnetic field is a bit higher than simulation results. That is because there are some water holes for the cooling circuit. The voltage applied to the magnet was 52.6 V. The power consumption was 25.0 kW. This power consumption was obtained after the solenoid reached stable state. In fact, when testing the gyrotron in the lab, the solenoid was running continuously at least 2 h, twice a day. The solenoid has been well cooled. We are confident that there is no risk for “thermal runaway.” The agreement between theory and experiment is good. Discrepancies might be explained by that the temperature of the copper foils is lower than expected.

Fig. 4 The photo of the solenoid



Fig. 5 The axial magnetic field profile of the solenoid



3 The Second Harmonic Gyrotron

The schematic of the second harmonic gyrotron with a 1.8 T solenoid is shown in Fig. 6. Two separated parts are split from the steel shell and fixed on the gyrotron tube. The diameter of the separated parts is slightly larger than the MIG.

Since the magnetic flux was concentrated into the cavity region, the distance between the cathode emitter and the cavity center is less than 80 mm. There is not enough space to use a gun coil to adjust the magnetic field in cathode region. Therefore, a more compact triode MIG was used to generate the gyrating electron beam in our present work. Another advantage of the triode MIG is its lower assembly accuracy requirement.

The optimized MIG geometry is shown in Fig. 7. The average radius of the emitter is 5 mm and the slant length is 1 mm. The tilt angle of the emitter is 40° . The average beam radius at the cavity entrance is 1.6 mm. A high pitch factor 1.6 and low longitudinal velocity spread less than 3% favorable for beam-wave interaction could be obtained.

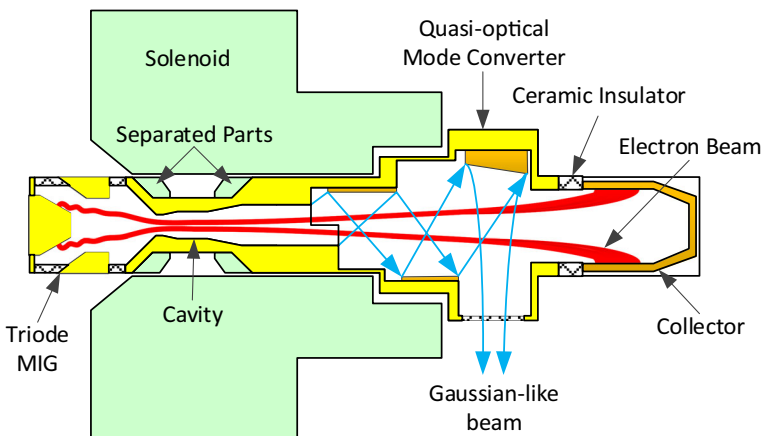
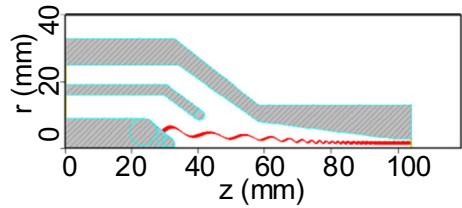


Fig. 6 The schematic of the gyrotron

Fig. 7 The optimized triode MIG geometry



The gyrotron with a conventional cylindrical cavity operates at the TE_{02} mode. The straight section of the cavity has a radius of 3.56 mm and a length of 25 mm, as shown in Fig. 8. According to the cold cavity theory, the diffraction Q factor of the cavity is about 2000, and the total Q factor is about 1600. The minimum start current of $TE_{0,2}$ mode in this cavity is about 0.8 A.

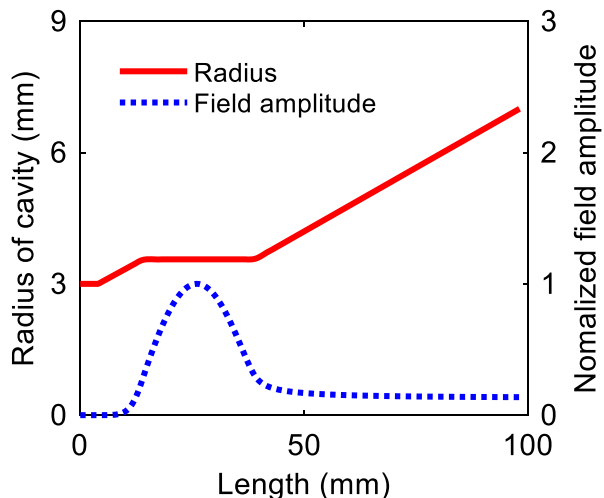
Following the method developed in [14], we designed a high-efficiency internal quasi-optical mode converter to separate the wave from the electron beam. The mode converter consists of a pre-bunch dimpled-wall launcher, a quasi-parabolic mirror, and two phase-correction mirrors. The main lobe of the launcher contains more than 98% power. The power flow density in the mode converter is shown in Fig. 9 and the electric field on the window surface is shown in Fig. 10. According to the simulation results, the mode conversion efficiency is 97%, and the Gaussian content of the output wave is 98%. The waist radius of the output beam at the window surface is 8 mm.

In order to enhance overall efficiency of the second harmonic gyrotron, a single-stage depressed collector was used. And the output window disk with a diameter of 60 mm is made of boron nitride (BN) ceramic.

4 Experimental Setup and Test Results of the Second Harmonic Gyrotron

The photo of the 94 GHz second harmonic gyrotron is shown in Fig. 11. The two separated carbon steel parts were brazed on the tube to concentrate the magnetic field into cavity region.

Fig. 8 The cavity radius and the normalized field amplitude in the cavity



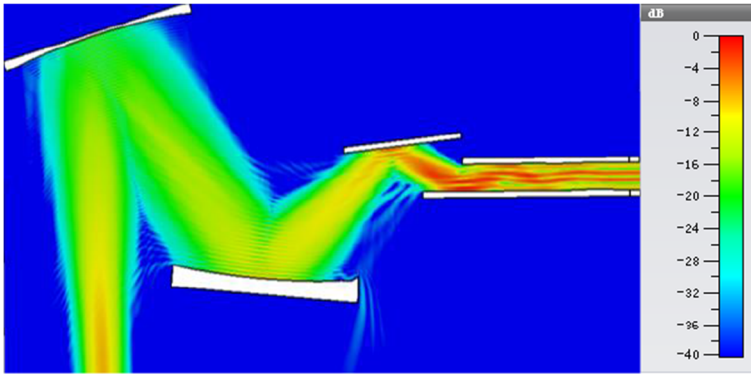


Fig. 9 Power flow density in the quasi-optical mode converter

Fig. 10 Electric field on the window surface

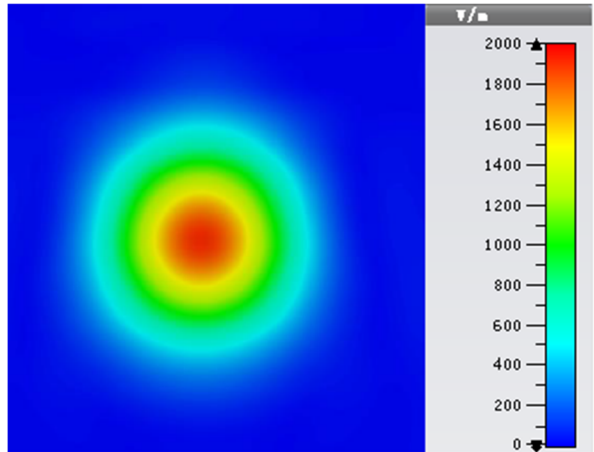


Fig. 11 (Left) The 94 GHz second harmonic gyrotron. (Right) The gyrotron and the 1.8 T solenoid on test platform

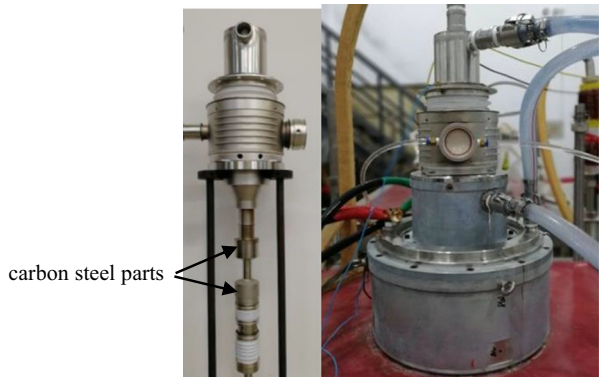
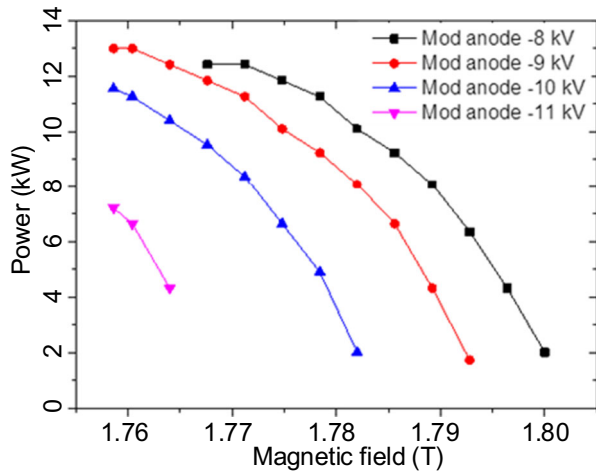


Fig. 12 Output power (pulse) of the second harmonic gyrotron with various mod-anode voltage conditions, the cathode voltage is -45 kV



The maximum diameter of the MIG is smaller than 66 mm. So, the gyrotron can be inserted into the solenoid, as shown in Fig. 11.

During the test, the mod-anode, cavity, dimpled-wall launcher, and the collector were cooled by water. The BN window disk is edge-cooled. In the test, a heterodyne receiver system was used to measure the gyrotron frequency. A water load was used to absorb and measure the output power.

During the pulse test with a duty ratio of 10%, when driven by a 45 kV, 1.6 A electron beam, 13 kW output power was obtained. The operating frequency is 94.08 GHz. The measured output power of the second harmonic gyrotron with various mod-anode voltage conditions is shown in Fig. 12. Figure 13 shows the thermal image on a heat-sensitive paper near the window captured in a single 10 ms pulse.

In the CW test, 5-min operation of the 94 GHz second harmonic gyrotron was successfully realized. Its operational frequency stabilized at a lower frequency of 93.9 GHz. That means the cavity was heated by the millimeter wave power. The output power of 12 kW was delivered by an electron beam of 45 kV, 1.6 A. And the output efficiency was 24% with a single-stage

Fig. 13 The thermal pattern of the window captured in a single pulse

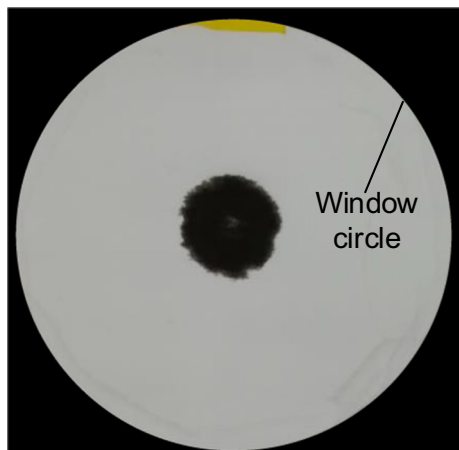
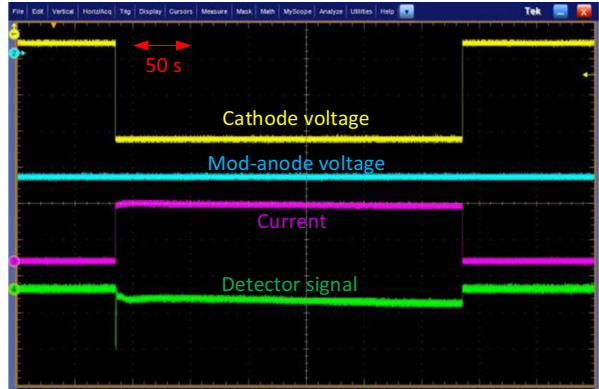


Fig. 14 Oscilloscope traces of the 5-min CW operation

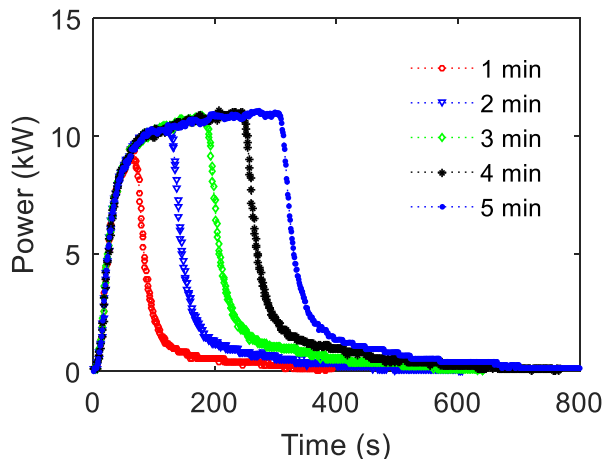


depressed collector with depressed potential of -14 kV (high negative voltage on the collector). The oscilloscope traces of the 5-min operation are shown in Fig. 14. The gyrotron was quite stable during the CW operation. At the beginning of the detector signal trace, a spike pulse signal was captured, that is probably because the detector system was disturbed. Figure 15 shows the water load calorimeter measurement results of the CW operations with 1 min, 2 min, 3 min, 4 min, and 5 min, respectively. It can be concluded that the operation of the second harmonic gyrotron is stable.

5 Summary

Continuous operation of a hard sealed, W-band, second harmonic gyrotron with a solenoid cooled by water was realized. The gyrotron is compact, with a length of less than 1 m. With the carbon steel shell, the magnetic field of the 1.8 T solenoid is self-shielding. Therefore, the gyrotron with the solenoid is suitable for vehicle platform. However, the power consumption of the 1.8 T solenoid is high and the output efficiency of the gyrotron is relatively low. Both the gyrotron and the solenoid could be improved to enhance overall efficiency.

Fig. 15 The water load calorimeter measurement results of the CW operations



Funding This work is financially supported by Ministry of Science and Technology of the People's Republic of China, National Key Research and Development Program under Grant No. 2016YFC0800308.

References

1. D. Lewis, M. A. Imam, L. K. Kurihara, A. W. Fliflet, A. Kinkead, Scott Miserendino, S. Egorov, R. W. Bruce, S. Gold, and A. M. Jung, "Material processing with a high frequency millimeter-wave source," *Mater. Manuf. Process.*, vol. 18, no. 2, pp. 151–168, 2003.
2. T. Idehara, I. Ogawa, K. Kawahata, H. Iguchi and K. Matsuoka, "Application of the Gyrotron FU II submillimeter wave radiation source to plasma scattering measurements," *Int. J. Infrared and Millim. Waves*, vol. 25, no. 11, pp. 1567–1579, 2004.
3. V. Erckmann, G. Dammertz, D. Dorst, L. Empacher, W. Forster, G. Gantenbein, T. Geist, W. Kasperek, H. P. Laqua, G. A. Muller, M. Thumm, M. Weissgerber, and H. Wobig, "ECRH and ECCD with high power gyrotrons at the Stellarators W7-AS and W7-X," *IEEE Trans. Plasma Sci.*, vol. 27, no. 2, 538–546, 1999.
4. M. Thumm, "High power gyro-devices for plasma heating and other applications," *Int. J. Infrared and Millim. Waves*, vol. 26, no. 4, pp. 483–503, 2005.
5. N. Kumar, U. Songh, T. P. Singh, and A. K. Sinha, "A review on the applications of high power, high frequency microwave source: gyrotron," *J. Fusion Energ.*, vol. 30, pp. 257–276, 2011.
6. S. Mitsudo, Aripin, T. Shirai, T. Matsuda, T. Kanemaki, and T. Idehara, "High power, frequency tunable, submillimeter wave ESR device using a gyrotron as a radiation source," *Int. J. Infrared Millim. Waves*, vol. 21, no. 4, pp. 661–676, 2000.
7. L. R. Becerra, G. J. Gerfen, R. J. Temkin, D. J. Single, and R. J. Griffin, "Dynamic nuclear polarization with a cyclotron resonance maser at 5 T," *Phys. Rev. Lett.*, vol. 71, no. 21, pp. 3561–3564, 1993.
8. T. Idehara, K. Kosuga, La Agus, I. Ogawa, H. Takahashi, M. E. Smith and R. Dupree, "Gyrotron FU CW VII for 300 MHz and 600 MHz DNP-NMR spectroscopy," *Int. J. Infrared Millim. Waves*, vol. 31, no. 7, pp. 763–774, 2010.
9. J. M. Neilson, M. Read and R. L. Ives, "Design and assembly of a permanent magnet gyrotron for active denial systems, in *Proc. of IEEE 11th Int. Vacuum Electron. Conf.*, Monterey, 2010, pp. 337–338.
10. D. Borodin, and M. Einat, "Copper solenoid design for the continuous operation of a second harmonic 95-GHz gyrotron," *IEEE Trans. Electron Devices*, vol. 61, no. 9, pp. 3309–3316, 2014.
11. M. Pilosof, and M. Einat, "95-GHz gyrotron with room temperature DC solenoid," *IEEE Trans. Electron Devices*, vol. 65, no. 8, pp. 3474–3478, 2018.
12. M. Pilosof, and M. Einat, "95 GHz gyrotron with water cooled magnet and high average power," in *Proc. 44th Int. Conf. Millim., Terahertz Waves (IRMMW-THz)*, 2019.
13. Sun Dimin, Zhuo Tingting, Ma Guowu, et al., "Recent Results of a CW, 94 GHz Second Harmonic Gyrotron Based on a Continuous Operation Solenoid," in *Proc. 44th Int. Conf. Millim., Terahertz Waves (IRMMW-THz)*, 2019.
14. A. V. Chirkov, G. G. Denisov, M. L. Kulygin, et al., "Use of Huygens' principle for analysis and synthesis of the fields in oversized waveguides," *Radiophys. Quantum Electron.*, vol. 49, no. 5, 344–353, 2006.

Publisher's Note Springer Nature remains neutral with regard to jurisdictional claims in published maps and institutional affiliations.